

## MEASUREMENTS OF THE AIRFLOW ABOUT A 1/64 SCALE FFG-7 FRIGATE MODEL AND CORRELATION WITH FULL SCALE RESULTS

N. MATHESON

Air Operations Division, Aeronautical Research Laboratory, DSTO  
506 Lorimer St, Fishermens Bend, VIC 3207, AUSTRALIA

### ABSTRACT

Low speed wind tunnel flow visualisation studies and velocity measurements have been made to identify features of the airflow about the helipad at the stern of a 1/64 scale model of a RAN FFG-7 class frigate at yaw angles from 0° to 180°. The data will be used in a computer code to simulate the behaviour of a Seahawk helicopter operating from the helipad. Some important features of the flow are presented and related to the operation of the helicopter from the flight deck. Velocity measurements on the model are also compared with some full scale results above the helipad.

### NOTATION

U	Freestream reference velocity in wind tunnel
$u, v, w$	Velocities along the X, Y, Z, axes respectively.
$u_c$	crossflow velocity, $(v^2 + w^2)^{1/2}$
$u_{xy}$	Velocity component in xy plane, $(u^2 + v^2)^{1/2}$
X, Y, Z	Wind axes; X axis parallel to tunnel free-stream (+ve downstream), Y axis horizontal (+ve to tunnel stbd), Z axis vertical (+ve up).

### 1. INTRODUCTION

A computer model to simulate the dynamic flight behaviour of a Seahawk helicopter operating from the helipad of the FFG-7 class guided missile frigate is being developed at the Aeronautical Research Laboratory by Arney et al. (1991). The code will be used to analyse operational difficulties and to investigate flight envelope limits. The flight deck is at the stern where the airflow can be highly non-uniform due to the superstructure. This disturbed airflow is highly configuration dependent and it can adversely affect helicopter handling and performance during take-off and landing so that the flight envelope has to be restricted, as discussed by Hofman and Fang (1984). The velocity distribution of the airflow about the helipad is part of the data input needed for the computer code.

To provide the velocity data needed, a model of the ship was tested in the 2.7m x 2.1m test section of the Low Speed Wind Tunnel at ARL. Initially, flow visualisation studies were made to identify the main features of the flow, followed by mean flow velocity measurements about the helipad. Measurements were also made above the helipad of HMAS Darwin fitted with stabilisers to provide data on a full scale ship.

### 2. SHIP, WIND TUNNEL MODEL, AND EQUIPMENT

#### 2.1 Ship and Wind Tunnel Model

A very detailed 1/64 scale model of the above waterline portion of the hull, shown on a ground-board across the test section in Figure 1, was used for the wind tunnel tests.

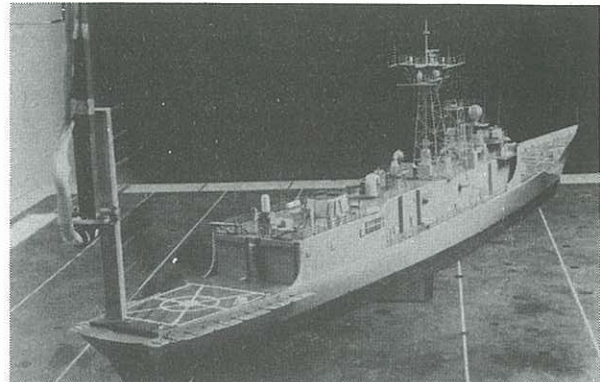


Fig.1 FFG-7 model and yaw probes in the tunnel.

The ship has a length of 138.1m (2.158m model scale) and a breadth of 14.3m (0.224m model scale). The helipad is 24.9m long, 14.1m wide at the hangar doors and 10.6m wide at the stern. The Seahawk helicopter is 19.8m long and it has a rotor diameter of 16.4m at a height of 3.5m. The upper deck is 5.6m above the helipad. These dimensions show the small size of the helipad in relation to the Seahawk.

The velocity measurements were made on a model of the ship which had a 2.44m extension to the deck just above the waterline at the transom, with a step-down of 0.6m from the helipad, shown in Figure 1, but the flow visualisation studies were made on a model of the early version of the ship before this extension was added.

Boundary layer effects from the groundboard were minimised by placing a 45mm spacer under the model. The earth's boundary layer and funnel plume effects were not simulated, and ship motion dynamic effects such as heave, pitch and roll were not included.

#### 2.2 Flow Visualisation Methods

A single tuft at the end of a long rod, and a single smoke probe were moved around the helipad by hand. A mixture of kerosene and french chalk was used for the surface flow visualisation tests. The flow patterns were recorded simultaneously using 3 video cameras, on the side, top, and aft of the test section. Flow features were also recorded with still cameras in the same locations.

#### 2.3 Model Velocity Measuring Equipment

A rake of 'six-hole' pyramid head velocity vector probes was used to measure the 3-dimensional mean velocity distributions around the helipad. The rake has 8 probes 50mm apart which were aligned along the tunnel longitudinal axis during the tests. The probes were calibrated simultaneously at pitch and sideslip angles

each ranging from  $-30^\circ$  to  $+30^\circ$ . The rake was mounted on a carriage and traversed across the tunnel using a microprocessor controlled stepper motor and leadscrew, with the probes in the vertical plane, shown in Figure 1. The carriage was mounted on linear bearings and rails on the tunnel ceiling and moved fore and aft manually. Probe and tunnel reference pressures were measured using a PSI model 8400 electronic scanning system and an IBM PS/2-80 computer that allowed the pressures to be measured at up to 20,000 readings/sec.

#### 2.4 Full Scale Ship Airwake Measuring Equipment

The airwake was measured using 3 sets of triaxial propeller-vane anemometers. The three anemometers in each set measured the longitudinal, lateral, and vertical velocity components at a given location. They were attached to a vertical mast to measure the air velocity at heights of 3.2m, 6.4m and 9.6m above the helipad. The mast was moved around the deck on wheels.

Reference airspeeds were measured at the top of the mainmast and at the sides and rear of the helipad. Heading and speed were recorded from the ships' instrumentation. The motion of the flight deck was measured using a tri-axial accelerometer pack and rate gyroscopes, so the airwake data could be converted to other frames of reference, Hourigan et al. (1991).

### 3. TEST CONDITIONS

#### 3.1 Model Flow Visualisation and Airwake Conditions

The flow visualisation tests were made at yaw angles of  $0^\circ$ ,  $\pm 15^\circ$ ,  $\pm 30^\circ$ ,  $\pm 60^\circ$ ,  $\pm 90^\circ$ ,  $\pm 135^\circ$  and  $180^\circ$ . Both +ve and -ve angles were tested as there was a small asymmetry in the superstructure amidships where the lifeboat was carried on the port side. Owing to the very small asymmetry effects the velocity tests were only made at yaw angles with the bow to starboard. The velocity tests were made at 50.0 m/s (97 kn), and the flow visualisation tests were made over a range of speeds. The velocity measurement envelope was selected to cover the approach and landing paths normally used in ship operations. Figure 2 shows a typical grid pattern for the velocity measurements at  $30^\circ$  yaw. The origin of the axis system is on the centreline directly in front of the hangar door, at a height of 20 mm (1.3m full scale) above the deck. The grid is about 5 rotor diameters wide and 6 rotor diameters long. Velocity measurements were taken at heights up to 22.4m (350mm model scale) above the origin.

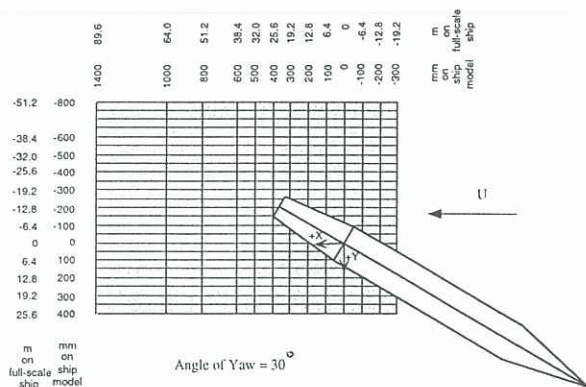


Fig.2 Velocity measurement grid for model at  $30^\circ$  yaw.

#### 3.2 Full Scale Airwake Test Conditions

Unusually calm conditions occurred during the trial so that the tests could only be carried out over a limited range of wind velocities of:

10,20,35 kn at  $0^\circ$  and  $30^\circ$  yaw angle  
 10,20 kn at  $60^\circ$  and  $90^\circ$  yaw angle  
 10 kn at  $135^\circ$  and  $180^\circ$  yaw angle

The velocity measurements were taken at 13 relatively evenly spaced locations on the flight deck at heights of 3.2m, 6.4m, and 9.6m, giving a total of 39 measurement positions above the deck for each relative wind velocity. It was not practicable to measure velocities outside the deck area.

### 4. MODEL RESULTS

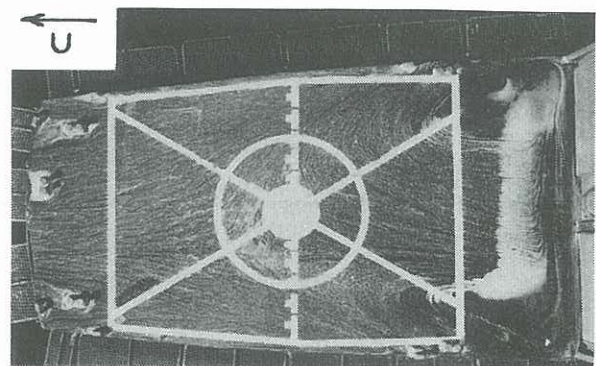
Only a small number of examples of the flows for operation at some of the more common yaw angles of  $0^\circ$ ,  $30^\circ$  and  $90^\circ$  are given.

#### 4.1 Model at $0^\circ$ Yaw Angle

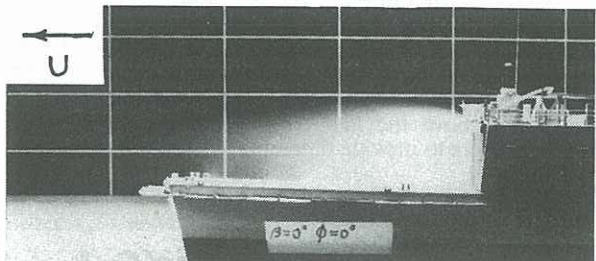
Major features of the flow are given in Figures 3 and 4. The surface flow pattern in Figure 3(a) illustrates the complexity of the flow which separates from the upper deck and each side of the hangar to form a separation bubble extending to the centre of the helipad, as shown in Figure 3(b), with reverse flow close to the deck. The surface pattern shows two trailing vortices at the junctions of the hangar wall and the flight deck, one rotating anticlockwise on the port side and the other rotating clockwise on the starboard side, when looking upstream. These vortices are weak and they dissipate rapidly as shown by the crossflow vectors near the stern in Figure 4(c).

The axial velocity contours,  $u/U$ , just at the end of the helipad at  $x = 500$ mm (32m full scale) and far downstream at  $x = 1400$  mm (90m full scale), in Figures 4(a) and (b) respectively, show the high shear in the wake that persists well downstream. Figure 4 shows that the wake behind the hangar, the mainmast, and the funnel extends about 350 mm (22 m full scale) above the helipad. The wake is turbulent and there is a small downward velocity component that extends well above the helipad, as shown in Figures 3(b) and 4(c).

Unless corrective action is taken by the pilot this small downward flow could cause a slightly harder landing than normal. In addition, operation in the wake

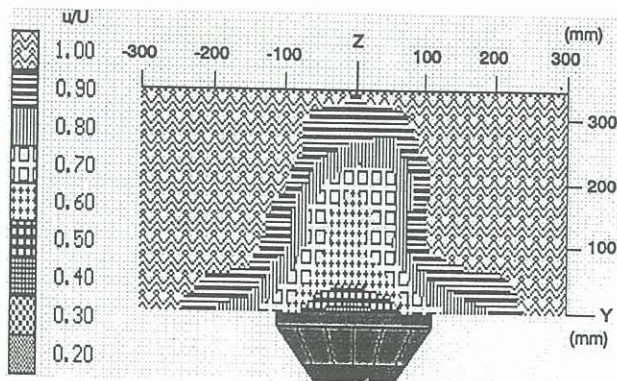


3(a) Surface flow pattern

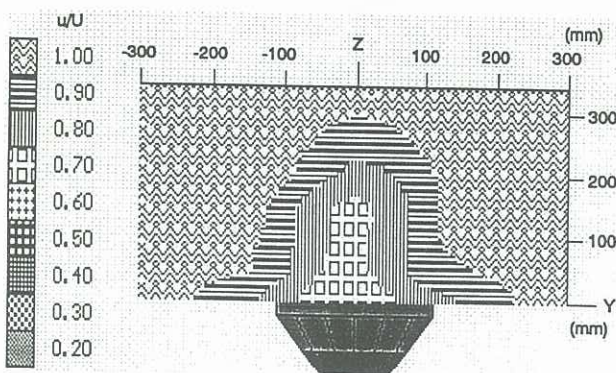


3(b) Separation behind hangar doors

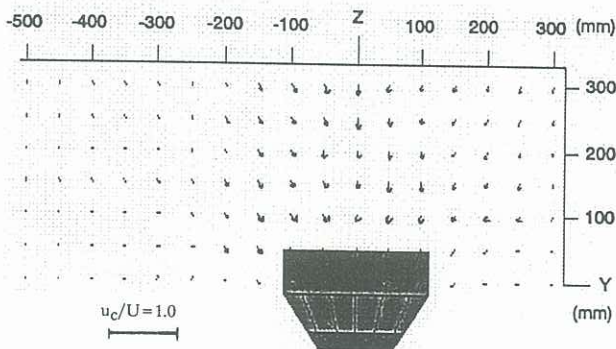
Fig. 3 Flow visualisation at  $0^\circ$  yaw



4(a) Axial velocity contour  $u/U$  at  $x=500$  mm



4(b) Axial velocity contour  $u/U$  at  $x=1400$  mm



4(c) Crossflow velocity vectors  $u_c/U$  at  $x=500$  mm

Fig. 4 Velocity distribution at  $0^\circ$  yaw

will result in 'drafting' and the helicopter could move forward unexpectedly towards the hangar. Operation across the wake could cause further handling problems.

#### 4.2 Model at $30^\circ$ Yaw Angle

Some features of the flow are shown in Figures 5 and 6. Although not shown, the flow separates directly behind the hangar doors with reverse flow close to the deck from the centre of the helipad, in a similar way to the flow at  $0^\circ$  yaw. The superstructure produces a large strong vortex on the leeward side of the hull, shown by the cross flow vectors in Figure 6 (a) and 6(b), which rotates in a clockwise direction when looking upstream. The centre of the vortex is near the mid height of the hangar doors and it slowly rises as it moves aft near the leeward side of the hull before moving downstream directly behind the stern as shown in Figure 6(b). The vortex produces significant lateral velocity components as well as a large upward component at the leeward edge of the helipad, as shown in Figures 5 and 6(a), and a

similar downwash component further to the leeward side. The axial velocity contours,  $u/U$ , in Figures 6(c), show that high shear still exists in the wake far downstream similar to the  $0^\circ$  yaw case.

Operating a helicopter in the vortex wake could cause significant handling problems. Drafting could occur in the same way as at  $0^\circ$  yaw, and the high upwash and downwash velocity components into the rotor disc will cause the helicopter to pitch and roll, as well as

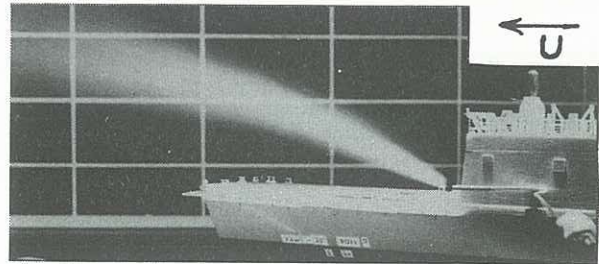
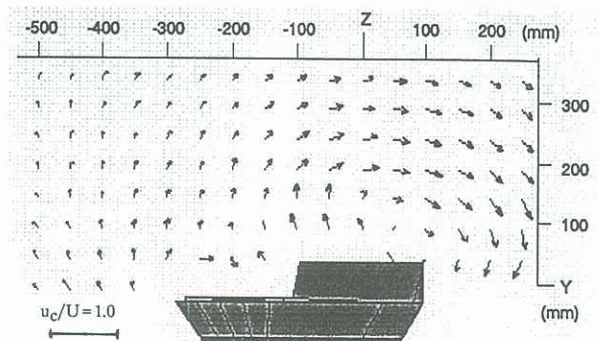
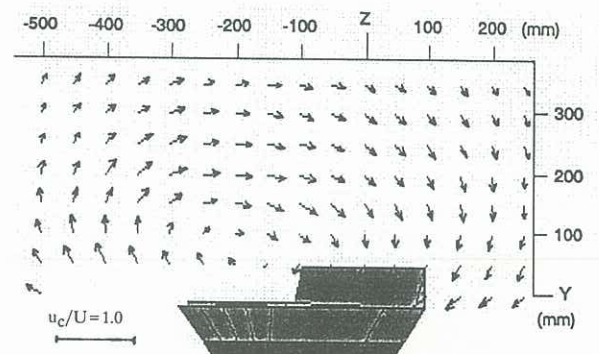


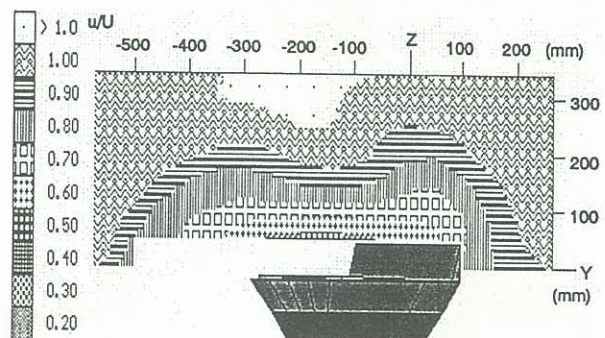
Fig. 5 Upflow at leeward edge of helipad at  $30^\circ$  yaw.



6(a) Crossflow velocity vectors  $u_c/U$  at  $x=500$  mm



6(b) Crossflow velocity vectors  $u_c/U$  at  $x=1400$  mm.



6(c) Axial velocity contour  $u/U$  at  $x=1400$  mm

Fig. 6 Velocity distribution at  $30^\circ$  yaw.

move laterally and vertically, so that it is even more difficult to control compared with the  $0^\circ$  yaw case.

### 4.3 Model at $90^\circ$ yaw angle

The main features of the flow are shown in Figures 7 and 8. The flow separates from the upstream edge of the helipad and hangar. There is also a large upwash near the upstream side of the helipad and a similar downwash on the downstream side where the flow is turbulent, as shown in Figure 7. The downwash persists well downstream as shown in Figure 8(a), but the wake is much less significant than at  $0^\circ$  and  $30^\circ$  yaw.

If the helicopter approaches the helipad from either side the upwash and downwash in these regions could cause some handling problems, but little difficulty is expected if the approach is made directly towards the stern in line with the ship's heading.

## 5. MODEL AND FULL SCALE SHIP COMPARISON

An example of the full scale ship and model correlation for  $30^\circ$  yaw and a ship speed of 35 kn is given

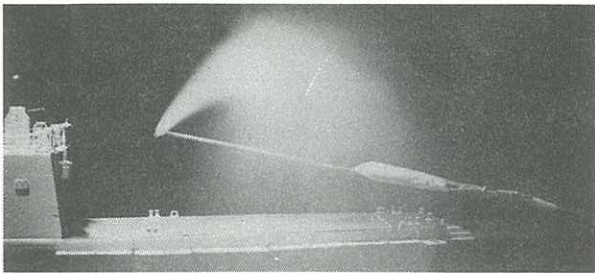
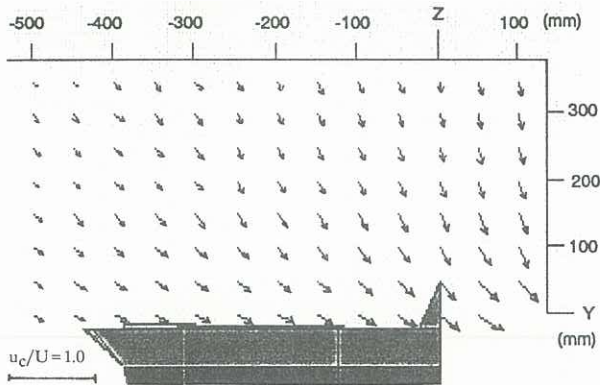
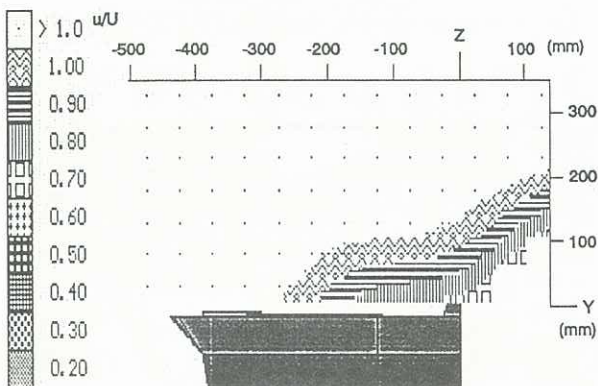


Fig. 7 Flow visualisation at  $90^\circ$  yaw, looking upstream



8(a) Crossflow velocity vectors  $u_c/U$  at  $x = 1400$  mm



8(b) Axial velocity contour  $u/U$  at  $x = 1400$  mm

Fig. 8 Velocity distribution at  $90^\circ$  yaw.

in Figure 9. The mean velocities,  $u_{xy}/U$ , are shown in vector form in a plane 2.1m above the upper deck which corresponds to 6.4m (100mm model scale) above the axes origin. Corrections for the effects of ship motion have not been made yet, although these effects should be small due to the stabilizers and the calm test conditions.

The model and full scale results are in reasonable agreement. It is difficult to make a direct comparison because the results were not taken at exactly the same locations and because the yaw probes were not calibrated to measure high flow angles and very low velocities. However, where the results can be compared, for example at positions 1,5,6,7,11,12 and 13 they agree reasonably well. At positions 2,3,4,9 and 10, the results cannot be compared because the model results are outside the probe calibration limits.

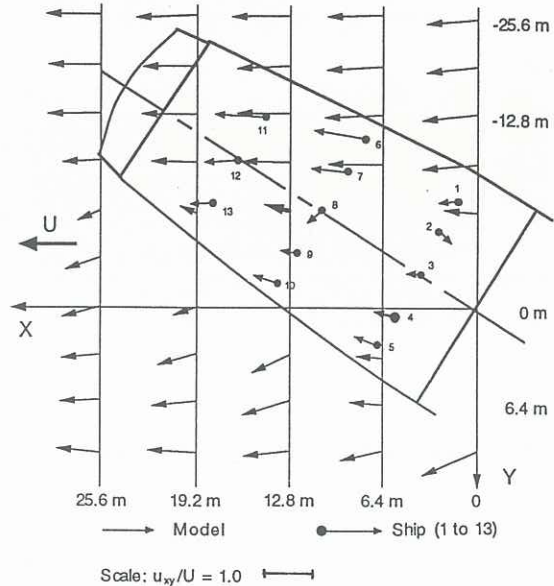


Fig.9 Velocity,  $u_{xy}/U$ , comparison for model and ship

## 6. CONCLUDING REMARKS

Wind tunnel tests and mean flow velocity measurements on a model showed that significant areas of separation, high flow angularity, vorticity, and unsteady flow existed near the helipad of a FFG-7 frigate which could have a major effect on the flight characteristics of a helicopter during take-off or landing. Mean velocity measurements above the helipad on the ship compare reasonably well with the model results.

## ACKNOWLEDGEMENTS

The Author would like to thank N. Gilbert, C. Sutton, J. Hodges, A. Arney, Y. Link, D. Carnell and C. Heinze from ARL, for their contributions to this work.

## REFERENCES

1. Arney, A.M., Blackwell, J., Erm, L.P. and Gilbert, N.E. (1991). A Review of Australian Activity on Modelling the Helicopter/Ship Dynamic Interface. AGARD Conference Proceedings 509, (Aircraft Ship Operations), Paper 20, Seville, Spain, November 1991.
2. Hofman, C.F.G.M. and Fang, R. (1984). Determination of Limitations for Helicopter Ship-borne Operations. Report NLR MP 84072, National Aerospace Laboratory, The Netherlands.
3. Hourigan, D.T., Sutton, C.W. and Bird, F.J. (1991). Instrumentation for Airwake Measurements on the Flight Deck of a FFG-7. Tech Memo 450, Flight Mechanics Branch, Aeronautical Research Laboratory.